

Investigation of Cure Kinetics and Storage Stability of the *o*-Cresol Novolac Epoxy Nanocomposites with Pre-intercalated Phenolic Hardeners

Tae Yong Hwang and Jae Wook Lee*

Applied Rheology Center, Dept. of Chemical and Biomolecular Engineering, Sogang University, Seoul 121-742, Korea

Sang Min Lee

R&D Center, Kolon Industries, Inc., Incheon 404-250, Korea

Gi Joon Nam

R&D Center, LS Cable, Ltd., Gyeonggi 431-831, Korea

Received August 18, 2008; Revised September 23, 2008; Accepted September 24, 2008

Abstract: The cure kinetics of the epoxy-layered, silicate nanocomposites were studied by differential scanning calorimetry under isothermal and dynamic conditions. The materials used in this study were *o*-cresol novolac epoxy resin and phenol novolac hardener, with organically modified layered silicates. Various kinetic parameters, including the reaction order, activation energy, and kinetic rate constants, were investigated, and the storage stability of the epoxy-layered silicate nanocomposites was measured. To synthesize the epoxy-layered silicate nanocomposites, the phenolic hardener underwent pre-intercalation by layered silicate. From the cure kinetics analyses, the organically modified layered silicate decreased the activation energy during cure reaction in the epoxy/phenolic hardener system. In addition, the storage stability of the nanocomposite with the pre-intercalated phenolic hardener was significantly increased compared to that of the nanocomposite with direct mixing of epoxy, phenolic hardener, and layered silicate. This was due to the protective effect of the reaction between onium ions and epoxide groups.

Keywords: cure kinetics, nanocomposites, layered silicates, *o*-cresol novolac epoxy, phenol novolac.

Introduction

Epoxy resin is a thermosetting polymer, which is necessary to be cured from a pre-polymeric state to a three dimensional network structure to show its superior performance. The mechanism and kinetic study is one of the basic researches not only for epoxy resin but also nanocomposite, and has been widely investigated.¹⁻⁷ Because the cure of epoxy resin involves various chemical reactions, the structures and performances of the cross-linked network can be significantly influenced by the properties of curing agents and curing conditions.

For the epoxy polymer layered silicate nanocomposites (PLSN), surface modification of the layered silicates by the organo-functional group (so called 'intercalants') is essential to improve the interfacial interaction or compatibility between the layered silicates and the matrix polymers. The most popular organo-functional group for surface treatment is based on onium ions, which contain an amine cations and long hydrocarbon chains. In the epoxy PLSN system, the

presence of organic compounds may affect the cure of epoxy PLSN, and then simultaneously may be influenced on the cured performances, whereas the layered silicates with wide surface area at a molecular scale may inhibit the cure reaction by the steric hindrance. This causes the storage stability problem which obstructs the commercialization of epoxy layered silicates nanocomposites. To solve this problem, the pre-intercalated indirect synthesis method in epoxy PLSN was introduced in this study.^{8,9}

The effect of primary amine based intercalants on the cure reaction of epoxy resins was explained by Lan's group.¹⁰ Also, Kommann's group discussed about the steric effects of layered silicates on the intercalated epoxy PLSN.^{11,12} They found out that there is a competition between the intercalation rate and the cure reaction rate. However, there have been few investigations of the influences of intercalant on the curing mechanism and kinetics. Generally, the competition between the intercalation rate and the cure rate may vary depending upon the hardener type as well as cure temperature. Also, the competition is influenced by the type of clay and its chemical affinity with the given epoxy resin.

A variety of experimental techniques such as chromatog-

*Corresponding Author. E-mail: jwlee@sogang.ac.kr

raphy, differential scanning calorimetry (DSC), infrared spectroscopy, nuclear magnetic resonance spectroscopy, etc. have been developed to measure the changes of the chemical or physical properties to describe the cure reaction.¹²⁻¹⁵ Among these various techniques, DSC measurement was known as the most commonly adopted technique, though there are some different views in the literature concerning about the interpretation of the isothermal and the dynamic results obtained from DSC results.^{16,17}

Various rate expressions have been proposed in the literature for the cure reaction of the thermosetting polymer. It is often described in terms of n^{th} -order or autocatalytic mechanism.^{18,19} The n^{th} -order model is described as

$$d\alpha/dt = k(1-\alpha)^n \quad (1)$$

where α is the conversion, n is the reaction order, and k is the reaction rate constant. In this equation, the temperature dependency is usually expressed by the Arrhenius equation;

$$k = k_0 \exp(-E_a/RT) \quad (2)$$

where E_a is the activation energy, R is the gas constant, k_0 is the pre-exponential factor, and T is the temperature.

Generalized autocatalytic reaction is expressed as follows;

$$\begin{aligned} d\alpha/dt &= (k_1+k_2\alpha^m)(1-\alpha)^n \\ k_1 &= k_{10} \exp(-E_{a1}/RT) \\ k_2 &= k_{20} \exp(-E_{a2}/RT) \end{aligned} \quad (3)$$

where m and n are the reaction orders that are dependent on the temperature, and k_1 and k_2 are the reaction rate constants with Arrhenius temperature dependency. This model has been widely applied to describing the cure kinetics of epoxy, unsaturated polyester, and other thermosetting resins.^{20,22}

In order to determine the evolution of the cure for modeling, the cumulative exothermic heat (ΔH_t) evolved at time t during the DSC scan is assumed to be proportional to the degree of cure conversion α in the system. Provided that the cure reaction is the only thermal event and the specific heat capacity of the resins remains constant, the degree of cure α at time t can be obtained from the DSC scan based on the following equation;

$$\alpha = (\Delta H_t) / (\Delta H_T) \quad (4)$$

where ΔH_T is the total heat of cure, which is determined by the non-isothermal scanning in order to ensure the completed cure reaction.

The main purpose of this study was to understand the effect of organically modified layered silicates on the cure kinetics in the o-cresol novolac epoxy (CNE) resins quantitatively. The layered silicates were well intercalated in the phenolic hardener in advance before the cure reaction occurs. Also, the storage stability of CNE PLSN prepared by the pre-intercalated phenolic resin was investigated with the directly synthesized epoxy PLSN and the neat epoxy

materials.

Experimental

Materials and Sample Preparation. The epoxy resin used in this study was the commercialized o-cresol novolac epoxy (CNE, YDCN-500-4P) supplied from Kukdo Chemical Co., South Korea. The epoxy equivalent weight was 204 g/eq. The phenol novolac (PN) used in this study as an epoxy hardener was commercialized phenol novolac (KPE-F2000) supplied from Kolon Industries, Inc., South Korea. The layered silicate was the dimethyl benzyl hydrogenated tallow quaternary ammonium modified montmorillonite from Southern Clay Products (Cloisite 10A) with a cation exchange capacity (CEC) of 125 meq/100 g. The amount of layered silicate was controlled to 5 phr based on the total binder. The loading contents of epoxy resin and phenolic hardener was decided by stoichiometric mixing ratio. Triphenylphosphine (TPP) from Junsei Chemical Co. was used as catalyst without any further purification. TPP content was 0.5 phr for kinetics, and 0.1 phr for storage stability test based on total binders, respectively.

Two epoxy PLSNs and neat epoxy were prepared by pre-intercalation, direct intercalation, and simple melt synthesis: In pre-intercalation synthesis, PN resin was mixed with a desired amount of clays at 160 °C for 3 h in a kettle with a mechanical stirrer. Prepared pre-intercalated PN was degassed in a vacuum oven for 30 min at 160 °C, and poured into a stainless steel tray. CNE and pre-intercalated PN were melted separately in a forced convection oven at 120 °C for 1 h. The molten CNE and pre-intercalated PN were mixed together in a kettle and then mechanically stirred vigorously for 3 min. The mixture was poured into a stainless steel tray. In direct intercalation synthesis, CNE was initially mixed with the clay at 160 °C for 3 h in a kettle with a mechanical stirrer, and then the PN curing agent was added. The mixture was poured into a stainless steel tray. Moreover, to compare the kinetic effect of clay, CNE with PN hardener neat sample also was prepared by the procedures as described above except clays.

In this study, prepared samples were named according to the following notation. CNE-PN-A means the o-cresol novolac epoxy with pre-intercalated phenol novolac layered silicates nanocomposites. CNE-PN-AM indicates the PLSN prepared by direct intercalation method. Finally, CNE-PN means the neat sample without layered silicates.

The prepared samples were stored both in a refrigerator to keep their structures for kinetic study, and in a convection oven at 50 °C to accelerate the cure reaction for the storage stability test.

Thermal Characterization. Thermal properties, such as heat of cure, glass transition temperature (T_g), and curing time in dynamic and isothermal condition, were measured with a TA Instrument 2910 differential scanning calorimeter

(DSC).

Samples were capsulated in hermetic pans in a range of 5 to 7 mg. To detect the total heat of cure, we performed dynamic test. The heating rate was 10 °C/min from 20 to 300 °C. For the isothermal measurements, the temperatures were varied from 100 to 180 °C with an interval of 10 °C. The isothermally scanned samples were scanned again in dynamic mode to detect the residual heat of cure, and then rescanned dynamically to obtain their T_g 's.

All tests were repeated at least twice to verify the reproducibility of the measurements. Nitrogen gas was purged with a rate of 50 mL/min, and the temperatures and cell constants were calibrated with indium and zinc as reference materials.

Results and Discussion

DSC Measurements. Thermal analysis results of CNE-PN neat samples are listed in Table I. As the isothermal temperatures increase to 150 °C, increases of heat of cure are observed. However, the heat of cure was rapidly decreased at temperatures above 160 °C, and the results are presented in Figure 1. The changes of heat of cure according to the isothermal cure temperatures are caused by the vitrification process during curing, which interrupts the chemically controlled cure reaction. The cure rate expressions such as eq. (1) and eq. (3) are only effective during the chemically controlled cure reaction. Therefore, the cure kinetic analyses were carried out in ranges from 100 to 150 °C to avoid the frozen state, which shows relatively slow reaction after the vitrification compared to the chemically controlled cure reaction. The onset and peak times of the isothermal exothermic cure peaks are continuously decrease as the temperatures increase, though the vitrification is proceeding. This is because the vitrification is normally happened after the initial as well as middle steps of the reaction.

Figure 2 shows the results of the heat of cure obtained

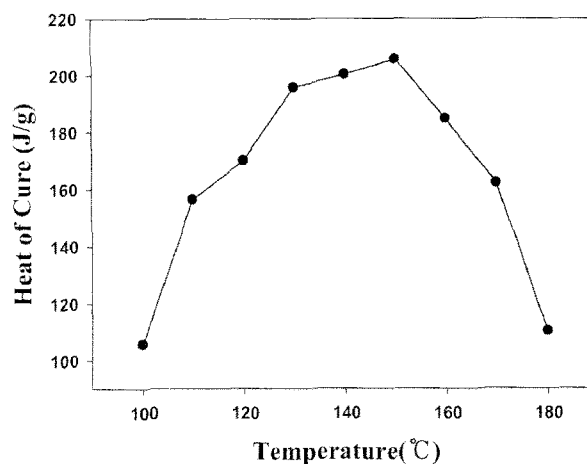


Figure 1. Heat of cure for CNE-PN neat samples obtained from isothermal scanning of DSC.

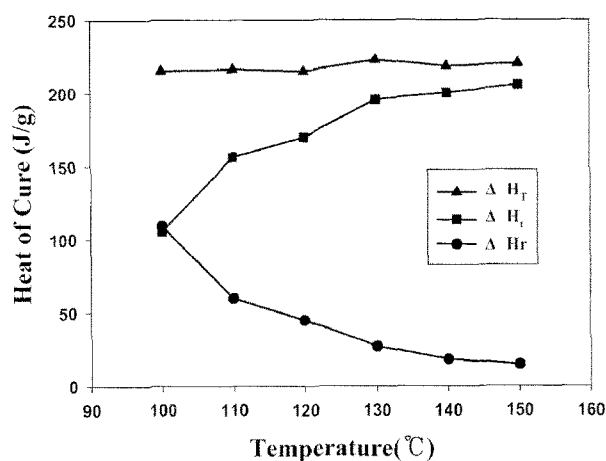


Figure 2. Isothermal (ΔH_i), residual (ΔH_r), and ultimate heat of cure (ΔH_T) for CNE-PN.

from the first isothermal scans, residual heat of cure measured by the dynamic scan after the first scan, and their

Table I. Cure Behaviors of CNE-PN Neat Samples Obtained from DSC

Temp. (°C)	Heat of Cure (J/g)	Degree of Cure (%)	Cure Exotherm Onset Time (min)	Cure Exotherm Peak Time (min)	3rd Scan T_g (°C)
100	105.7	45.26	3.52	39.8	161.50
110	156.4	66.98	3.38	20.7	159.87
120	170.0	72.80	3.29	12.19	158.32
130	195.7	83.81	3.07	7.54	158.85
140	200.3	85.78	3.03	5.39	160.28
150	205.6	88.05	2.97	3.97	157.14
160	184.7	79.10	2.92	3.50	159.04
170	162.1	69.42	2.82	3.24	160.84
180	110.2	47.10	2.91	3.13	160.74
Dynamic	233.5	100.0	-	-	160.03

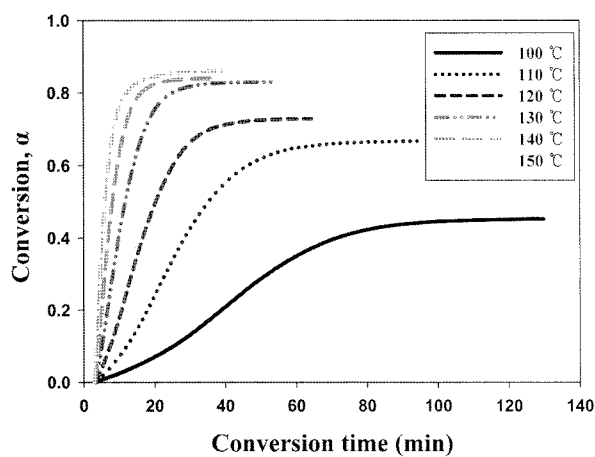
sums in temperature ranges from 100 to 150 °C. The heat of cure estimated from the first isothermal scan is gradually increased, whereas the residual heat of cure (ΔH_r) obtained from the second scan in dynamic mode is gradually decreases as the temperatures increase. However, the ultimate total heat of cure ΔH_T ($\Delta H_i + \Delta H_r$) shows no change in its quantity. It implies that the DSC scan results for CNE-PN are nicely matched with the theoretical evolution by the cure kinetics.

Cure Kinetics. The conversion α , which is the extent of curing reaction, can be calculated by the relationship between ΔH_T obtained from the dynamic scan and ΔH_i from the isothermal measurements in eq. (4). The estimated conversions of CNE-PN neat samples are presented in Figure 3(a) for the temperature ranges from 100 to 150 °C. The results of the CNE-PN-A samples are in Figure 3(b) in the temperature ranges from 130 to 180 °C. As shown in Figure 3(a), the degree of cure for CNE-PN neat samples did not reach to unity especially in low temperature conditions, whereas those of CNE-PN-A approached to unity for all temperature regions in Figure 3(b). It is believed that the

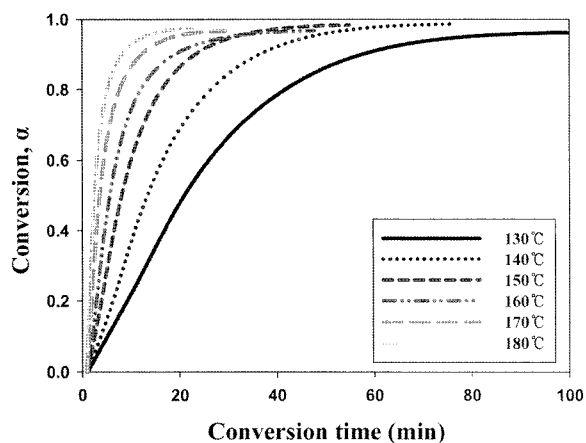
curing reaction was accelerated by onium ions on the layered silicates. Similar result was obtained by Dutta and Ryan about the effect of fillers on epoxy cure.²² They obtained that the conversion of filled system were higher than those of the neat system, which indicates that the filler could affect the cure kinetics.

The cure reaction rates as a function of temperature were calculated, and the results are shown in Figure 4(a) for the CNE-PN and in Figure 4(b) for the CNE-PN-A samples. Both CNE-PN and CNE-PN-A samples follow the autocatalytic reaction by showing that the conversion rates are zero at time $t=0$.

The conversion rates versus conversion for CNE-PN with temperatures are obtained and the results are presented in Figure 5. All Experimental data points are fitted by sigmoidal fitting analysis to calculate the reaction rate constant k_1 and k_2 , and the results of the CNE-PN samples are listed in Table II. They show highly reliable R^2 values for all temperature ranges. Arrhenius plots for k_1 , k_2 between rate constants and temperatures can be obtained from these reaction rate constants and the results are shown in Figure 6. It

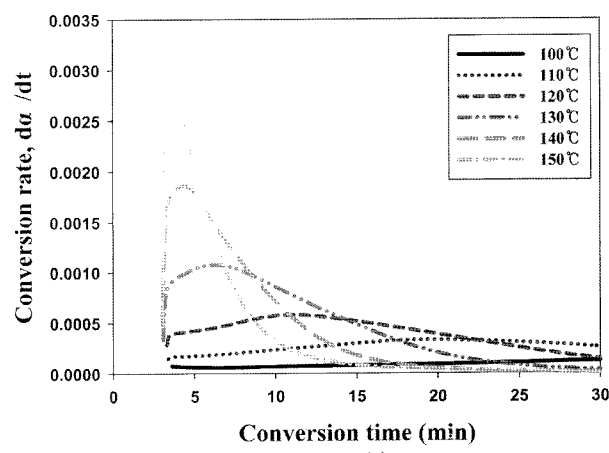


(a)

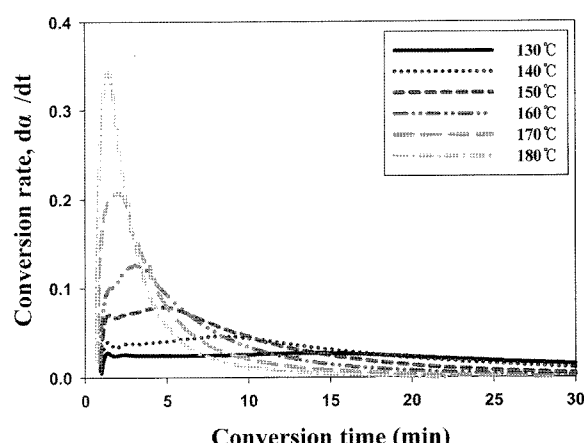


(b)

Figure 3. Conversion of CNE-PN (a) and CNE-PN-A (b) as a function of conversion.



(a)



(b)

Figure 4. Conversion rate of CNE-PN (a) and CNE-PN-A (b) as a function of time.

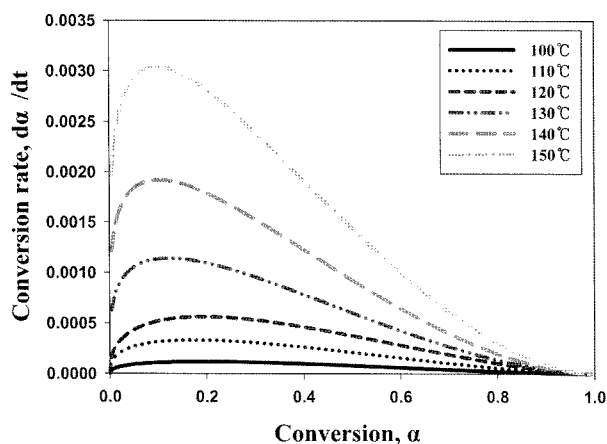


Figure 5. Conversion rate of CNE-PN as a function of conversion.

Table II. Cure Kinetic Parameters of CNE-PN Neat Samples

Temp. (°C)	K_1 (1/min)	K_2 (1/min)	R^2
100	0.00269	8.27E-4	0.9991
110	0.00731	0.00126	0.9968
120	0.01882	0.02006	0.9998
130	0.03876	0.04567	0.9995
140	0.08036	0.08587	0.9989
150	0.16898	0.16759	0.9969

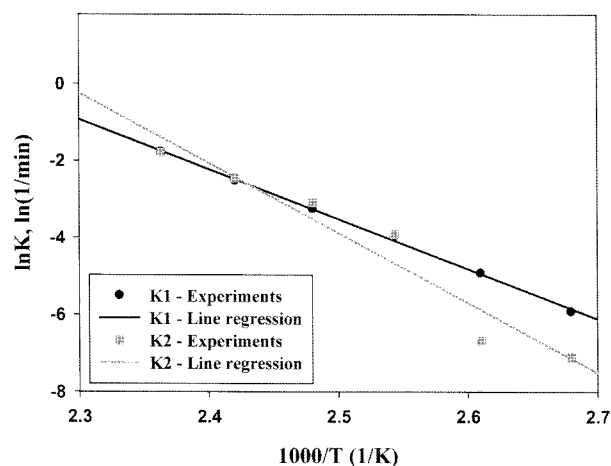


Figure 6. Arrhenius plot for CNE-PN neat samples.

reveals that k_{10} , k_{20} as well as E_{a1} , E_{a2} have relatively reasonable regression results. Also, the cure reaction rates as a function of conversion was obtained for the CNE-PN-A samples and the results are presented in Figure 7. The reaction constants for the CNE-PN-A samples were obtained by the same procedures mentioned above. The Arrhenius plot for CNE-PN-A is explained in Figure 8. The obtained kinetics parameters for the CNE-PN and CNE-PN-A were summarized in Table III. The activation energy of CNE-PN-A is

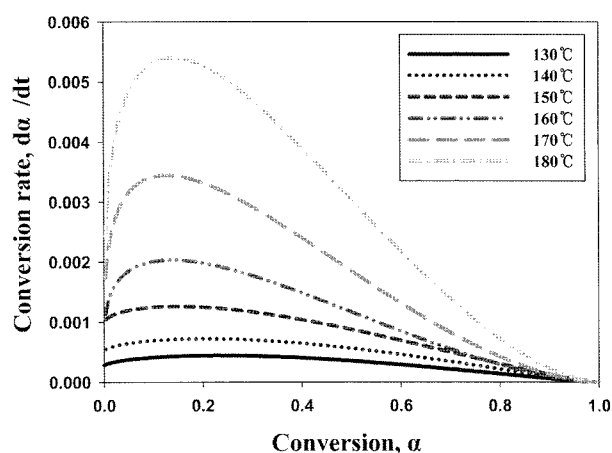


Figure 7. Conversion rates of CNE-PN-A as a function of conversion.

Table III. Kinetic Parameters of CNE-PN and CNE-PN-A Samples

	E_{a1} (KJ/mol)	E_{a2} (KJ/mol)	K_{10} (1/min)	K_{20} (1/min)
CNE-PN	107.54	151.01	3.285×10^{12}	1.093×10^{18}
CNE-PN-A	106.75	56.036	8.73×10^9	1.967×10^4

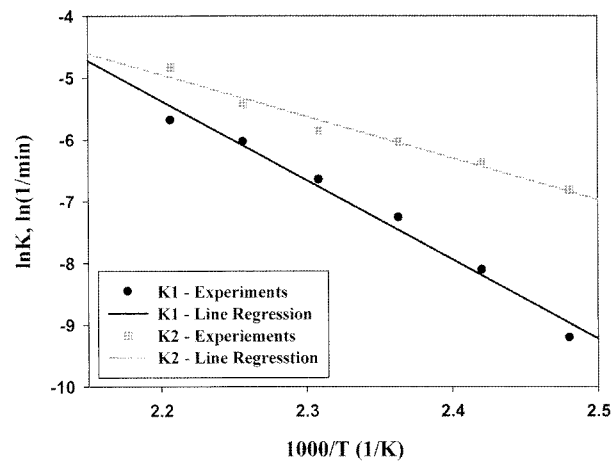
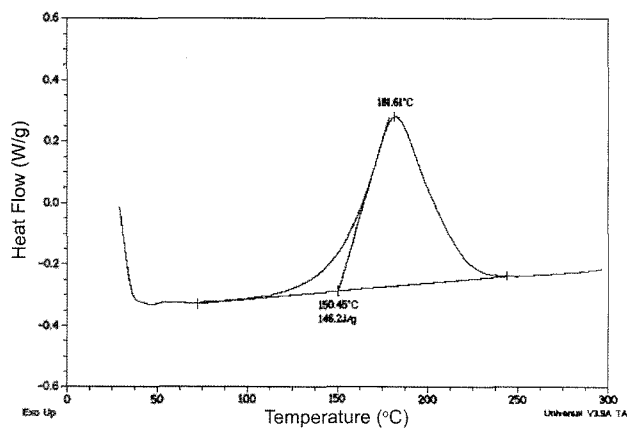


Figure 8. Arrhenius plot for CNE-PN-A samples.

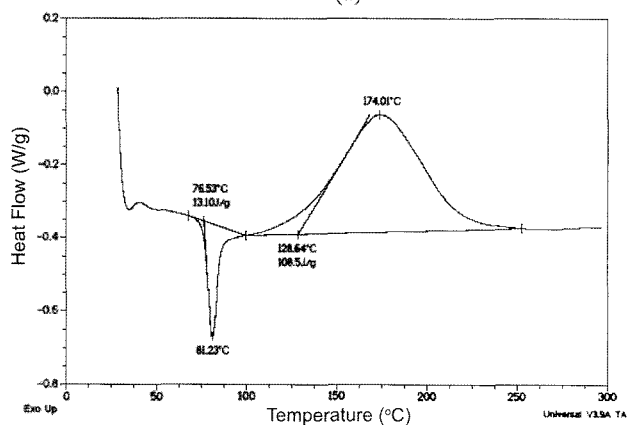
lower than that of CNE-PN neat samples. The decreased activation energy of PLSN implies that their reactions are accelerated by onium ions on the layered silicates, and lead the relatively rapid cure and the full conversions, whereas the reaction mechanism does not change.

Measurements of Storage Stability. To investigate the storage stability, three samples (CNE-PN, CNE-PN-A, and CNE-PN-AM) were stored at 50 °C for 50 days, and the heat of cure at initial and final stage were compared.

DSC thermograms of CNE-PN-A at initial and final stages are shown in Figure 9, and the results of the CNE-PN-AM



(a)

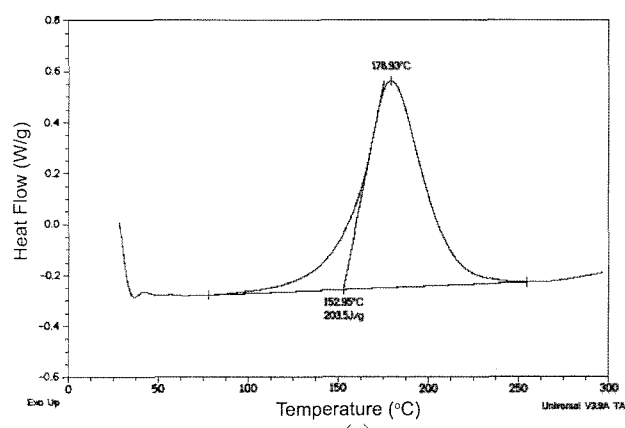


(b)

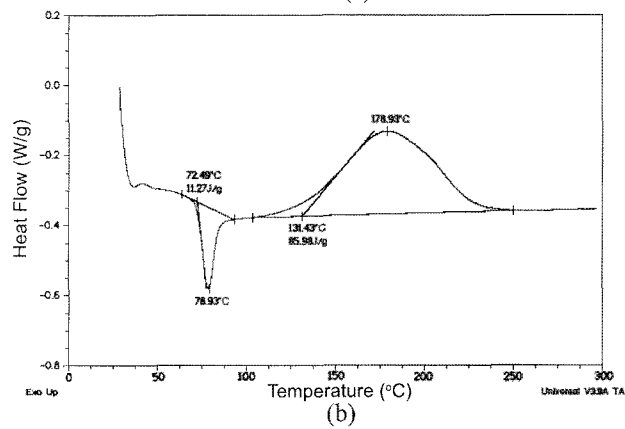
Figure 9. DSC thermogram of CNE-PN-A samples. (a) initial stage and (b) final stage.

are presented in Figure 10, respectively. In Figures 9 and 10, new endothermic peaks are observed at the final stage of the storage. These endothermic peaks represent the heat of melting of TPP catalysts which were recrystallized during the storage.

The changes of the heat of cure are listed in Table IV. The ratios of heat of cure between the initial and the final stage are also calculated. The CNE-PN-A sample shows higher storage stability with the heat of cure ratio of 74.2% than that of the CNE-PN-AM, directly synthesized PLSN with ratio of 41.7%, whereas the ratio of neat CNE-PN sample is 81.5%. The main cause of storage stability problem in epoxy layered silicate nanocomposites is the reaction between onium ion in layered silicate and epoxy group in polymer. Therefore, CNE-PN, neat polymer system without layered silicate, shows highest storage stability among them. The improvement of storage stability in CNE-PN-A can be explained by the steric hindrance effects of phenol resin molecules.⁸ The steric hindrance occurred by protecting the reaction between onium ions and epoxide groups by the pre-intercalated phenol molecules. Due to this protection, pre-intercalated PLSN showed better stability compared to the directly melt-intercalated PLSN.



(a)



(b)

Figure 10. DSC thermogram of CNE-PN-AM samples. (a) initial stage and (b) final stage.

Table IV. Storage Stabilities of Samples with Different Synthesis Methods

Type	Heat of Cure at the Beginning (A) (J/g)	Heat of Cure at the End (B) (J/g)	Heat of Cure Ratio (B/A, %)
CNE-PN-AM	203.5	85.98	41.73
CNE-PN-A	146.2	108.5	74.21
CNE-PN	139.5	113.6	81.49

Conclusions

Curing behaviors of CNE resins cured by both PN resins and pre-intercalated PN-A resins were studied by a DSC analysis under the isothermal and dynamic conditions. The curing was analyzed by the autocatalytic reaction kinetic equation. When we compared the activation energy of both composites, CNE-PN-A had lower value compared to CNE-PN. Moreover, the degree of cure for CNE-PN did not reach to unity, whereas that of CNE-PN-A reached almost unity. This was due to the acceleration of cure reaction by onium ions on the layered silicate. It led to the relatively rapid cure and the full conversion in CNE-PN-A. The storage stability was investigated for the pre-intercalated PLSN,

directly intercalated PLSN, and neat CNE-PN composites. When the changes of the heat of cure between the initial stage and final stage were measured, the changes in CNE-PN-A are smaller than that of CNE-PN-AM. The pre-intercalated CNE-PN-A increased the storage stability from 41.7% to 74.2% compared to the CNE-PN-AM. The improvement of storage stability is confirmed by steric hindrance between onium ions and epoxide groups by pre-intercalated phenolic molecules.

Acknowledgements. Financial support of the Applied Rheology Center (ARC), BK21 Education and Research Group, and the Special Grants of Sogang University are gratefully acknowledged.

References

- (1) M. E. Brown, *Introduction to Thermal Analysis*, Chapman & Hall, New York, 1988.
- (2) C. A. May, *Chemorheology of Thermosetting Polymers*, Maple Press, York, 1982.
- (3) H. F. Mark, N. Bikales, C. G. Overberger, G. Menqes, and J. I. Kroschwitz, *Encyclopedia of Polymer Science and Engineering*, John Wiley & Sons, New York, 1986.
- (4) M. T. Tonthat, T. D. Ngo, P. Ding, G. Fang, K. C. Cole, and S. V. Hoa, *Polym. Eng. Sci.*, **44**, 1132 (2004).
- (5) W. B. Xu, S. P. Bao, S. J. Shen, G. P. Hang, and P. S. He, *J. Appl. Polym. Sci.*, **88**, 2932 (2003).
- (6) J. D. Cho, Y. B. Kim, H. T. Ju, and J. W. Hong, *Macromol. Res.*, **13**, 362 (2005).
- (7) J. D. Cho, S. H. Kim, I. C. Chang, K. S. Kim, and J. W. Hong, *Macromol. Res.*, **15**, 560 (2007).
- (8) S. M. Lee, T. R. Hwang, Y. S. Song, and J. W. Lee, *Polym. Eng. Sci.*, **44**, 1170 (2004).
- (9) S. M. Lee, Ph.D. Thesis in Chemical and Biochemical Engineering, Sogang University, Korea (2004).
- (10) T. Lan, P. D. Kaviratna, and T. J. Pinnavaia, *J. Phys. Chem. Solid*, **57**, 1005 (1996).
- (11) X. Kommann, L. A. Berglund, and L. A. Berglund, *Polymer*, **42**, 1303 (2001).
- (12) X. Kommann, L. A. Berglund, and L. A. Berglund, *Polymer*, **42**, 4493 (2001).
- (13) E. Turi, *Thermal Characterization of Polymeric Materials*, Academic Press, New York, 1982.
- (14) P. Banks and R. H. Peters, *J. Polym. Sci. Part A: Polym. Chem.*, **8**, 2595 (1970).
- (15) M. G. Rogers, *J. Appl. Polym. Sci.*, **16**, 1953 (1972).
- (16) T. Ozawa, *J. Therm. Anal.*, **9**, 369 (1976).
- (17) A. M. Joven and C. C. Foun, *J. Appl. Polym. Sci.*, **32**, 3761 (1986).
- (18) M. R. Kamal and S. Sourour, *Polym. Eng. Sci.*, **13**, 59 (1973).
- (19) V. M. Gonzalezromero and N. Casillas, *Polym. Eng. Sci.*, **29**, 295 (1989).
- (20) B. R. Gebart, *J. Appl. Polym. Sci.*, **51**, 153 (1994).
- (21) J. Y. Lee, H. K. Choi, M. J. Shim, and S. W. Kim, *Thermochem. Acta*, **34**, 3111 (2000).
- (22) A. Dutta and M. E. Ryan, *J. Appl. Polym. Sci.*, **24**, 635 (1970).